Delft University of Technology

Gaussian Processes for Advanced Motion Control

Poot, Maurice; Portegies, Jim; Mooren, Noud; van Haren, Max; van Meer, Max; Oomen, Tom

DOI
10.1541/ieejjia.21011492

Publication date
2022

Document Version
Final published version

Published in
IEEJ Journal of Industry Applications

Citation (APA)
Poot, M., Portegies, J., Mooren, N., van Haren, M., van Meer, M., & Oomen, T. (2022). Gaussian Processes for Advanced Motion Control. *IEEJ Journal of Industry Applications*, *11*(3), 396-407. https://doi.org/10.1541/ieejjia.21011492

Important note
To cite this publication, please use the final published version (if applicable).
Please check the document version above.

Copyright
Other than for strictly personal use, it is not permitted to download, forward or distribute the text or part of it, without the consent of the author(s) and/or copyright holder(s), unless the work is under an open content license such as Creative Commons.

Takedown policy
Please contact us and provide details if you believe this document breaches copyrights.
We will remove access to the work immediately and investigate your claim.

This work is downloaded from Delft University of Technology.
For technical reasons the number of authors shown on this cover page is limited to a maximum of 10.

Green Open Access added to TU Delft Institutional Repository

'You share, we take care!' - Taverne project

https://www.openaccess.nl/en/you-share-we-take-care

Otherwise as indicated in the copyright section: the publisher is the copyright holder of this work and the author uses the Dutch legislation to make this work public.

IEEJ Journal of Industry Applications
Vol.11 No.3 pp.396–407 DOI: 10.1541/ieejjia.21011492

Invited Paper

Gaussian Processes for Advanced Motion Control

Maurice Poot[*a)] Non-member, Jim Portegies[**] Non-member
Noud Mooren[*] Non-member, Max van Haren[*] Non-member
Max van Meer[*] Non-member, Tom Oomen[*,***] Non-member

(Manuscript received Oct. 20, 2021, revised Dec. 14, 2021)
J-STAGE Advance published date : March 11, 2022

Machine learning techniques, including Gaussian processes (GPs), are expected to play a significant role in meeting speed, accuracy, and functionality requirements in future data-intensive mechatronic systems. This paper aims to reveal the potential of GPs for motion control applications. Successful applications of GPs for feedforward and learning control, including the identification and learning for noncausal feedforward, position-dependent snap feedforward, nonlinear feedforward, and GP-based spatial repetitive control, are outlined. Experimental results on various systems, including a desktop printer, wirebonder, and substrate carrier, confirmed that data-based learning using GPs can significantly improve the accuracy of mechatronic systems.

Keywords: gaussian processes, feedforward control, learning control

1. Introduction

Learning from data has traditionally been at the heart of mechatronic systems [(1)(2)] and has the potential to achieve future requirements regarding speed, accuracy, and functionality. Traditionally, mechatronic systems such as motion systems sample measurement data and process these in a digital environment to compute actuator inputs. These data are then used for learning dynamical models through system identification [(3)(4)], direct controller tuning based on data [(5)], as well as learning control [(6)]. The necessity to achieve future requirements in conjunction with the opportunities provided by a drastic increase in computation power and data from a large number of sensors has led to the recent development of new learning algorithms for motion control in mechatronic systems.

The accuracy, speed, and flexibility of motion determines the capabilities and market position of manufacturing equipment and scientific instruments. Examples include lithography [(7)], data-storage systems [(8)], industrial printing [(9)], advanced manufacturing [(10)], pick-and-place machines such as wirebonders and diebonders [(11)], and microscopy [(12)(13)]. Motion control, including feedforward and learning control, is a key technology enabling these machines to actually function, e.g., by realizing precise and fast motions that meet the demands of the market.

Increasing performance requirements in motion control of mechatronic systems lead to a situation where increasingly complex dynamical behavior needs to be compensated [(14)]. Flexible mechanical behavior leads to a situation where compliance is explicitly compensated for by snap feedforward [(15)], as well as position-dependent feedback [(16)]. At the same time, nonlinear friction and hysteresis aspects are being modeled and compensated for [(17)–(19)].

The use of data has always been key in tuning feedback and feedforward motion controllers, and had led to a large range of data-driven control and related system identification approaches. A large number of data-driven feedback algorithms have been developed, e.g., [(5)(20)], and implemented on motion systems [(21)(22)]. At the same time, major improvements have been made in the learning of dynamical models, i.e., system identification, for controller tuning, both nonparametrically [(23)] and parametrically, which is further extended towards position-dependent systems in [(24)]. Data-driven feedforward has been substantially developed, including repetitive control and learning control [(6)(25)(26)], and related disturbance observers for motion control [(27)]. These techniques have been further refined to enable the automated tuning of feedforward signals for a large class of tasks, including [(28)(29)], which have been further integrated with system identification algorithms [(30)].

In a different line of developments, Gaussian processes (GPs) have drastically impacted the recent theoretical development of system identification and learning to control. GPs have attracted substantial attention in machine learning, e.g., [(31)], see also [(32)] for relevant developments towards reinforcement learning. These have led to new ideas on the identification of linear models [(33)–(36)], frequency domain identification [(37)], integrated identification and learning [(38)(39)], data-driven feedback linearization [(40)], model predictive control [(41)(42)], robotic systems [(43)], wind turbine control [(44)], estimation [(45)], magnetic field mapping using SLAM [(46)], solving nonlinear optimal control problems [(47)], model uncertainty in

a) Correspondence to: Maurice Poot. E-mail: m.m.poot@tue.nl
* Control Systems Technology Section, Department of Mechanical Engineering, Eindhoven University of Technology
Eindhoven, The Netherlands
** CASA, Department of Mathematics and Computer Science, Eindhoven University of Technology
Eindhoven, The Netherlands
*** Delft Center for Systems and Control, Delft University of Technology
Delft, The Netherlands

© 2022 The Institute of Electrical Engineers of Japan.

safety-critical controllers [48], etc.

Although important theoretical developments have been made in the use of GPs in the broad area of identification and control, its use in advanced motion control of precision mechatronics has only recently been established. The aim and main contribution of this paper is to show the broad potential of GPs for motion control applications. In particular, applications to feedforward and learning control, which clearly benefit from the use of GPs, are outlined. Specific cases and an outline follow in Sec. 2.2.

Notation. The considered systems are discrete-time, single-input, single-output, and linear time-invariant, unless stated otherwise. Let $P(z)$ denote a transfer function, with z a complex indeterminate, q is the forward time-shift operator, i.e., $qx(t) = x(t+1)$, and $P(q)$ denotes the pulse-transfer operator associated with $P(z)$. The weighted 2-norm of a vector x is denoted as $\|x\|_W := \sqrt{x^\top W x}$, where W is a weighting matrix. Signals are often tacitly assumed of length N.

2. Advanced Motion Control

In this section motion control and feedforward control for advanced motion control applications is described. Moreover, the potential of GPs for different applications is highlighted.

2.1 Motion Control Mechatronic positioning systems consist of mechanics, actuators, and sensors [49][50]. The actuators typically generate forces or torques and are considered as input to the system. The sensors typically measure position or rotation and are considered outputs of the system.

In the frequency range that is relevant for control, the dynamical behavior is mainly determined by the mechanics. In particular, the mechanics can typically be described as [51]

$$G_m = \underbrace{\sum_{i=1}^{n_{RB}} \frac{c_i b_i^T}{s^2}}_{\text{rigid-body modes}} + \underbrace{\sum_{i=n_{RB}+1}^{n_s} \frac{c_i b_i^T}{s^2 + 2\zeta_i \omega_i s + \omega_i^2}}_{\text{flexible modes}}, \cdots\cdots (1)$$

where n_{RB} is the number of rigid-body modes, the vectors $c_i \in \mathbb{R}^{n_y}$, $b_i \in \mathbb{R}^{n_u}$ are associated with the mode shapes, and $\zeta_i, \omega_i \in \mathbb{R} \geq 0$. Here, $n_s \in \mathbb{N}$ may be very large and even infinite [52]. Note that in (1), it is assumed that the rigid-body modes are not suspended, i.e., the term $\frac{1}{s^2}$ relates to Newton's law. In the case of suspended rigid-body modes, e.g., in case of flexures as in [53][54], (1) can directly be extended.

In traditional positioning systems, the number of actuators n_u and sensors n_y equals n_{RB}, and are positioned such that the matrix $\sum_{i=1}^{n_{RB}} c_i b_i^T$ is invertible. In this case, matrices T_u and T_y can be selected such that

$$G = T_y G_m T_u = \frac{1}{s^2} I_{n_{RB}} + G_{\text{flex}}, \cdots\cdots\cdots\cdots\cdots\cdots (2)$$

where T_y is typically selected such that the transformed output y equals the performance variable.

The main goal in motion control is a servo task, i.e., let the output y follow a reference trajectory r, see Fig. 1. In particular, the goal is to minimize

$$e = Sr - SGf - Sv \cdots\cdots\cdots\cdots\cdots\cdots\cdots\cdots\cdots (3)$$

where

$$S = (I + GC)^{-1}. \cdots\cdots\cdots\cdots\cdots\cdots\cdots\cdots\cdots\cdots (4)$$

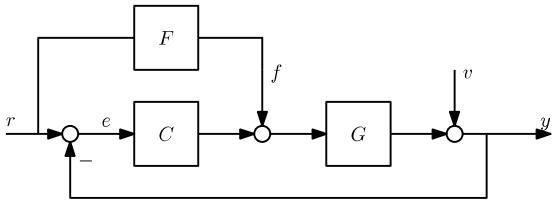

Fig. 1. Traditional motion control architecture

Typically, the reference is designed such that it is realizable without violating actuator constraints [55]. Throughout, it is assumed that the feedback controller C is fixed.

In many advanced motion control applications, the feedforward has by far the largest contribution [56], i.e., the signal f in Fig. 1 ensures e in (3) is small. The optimal tracking error in the sense of zero reference-induced tracking error, i.e., $S(r - Gf) = 0$, is obtained for a feedforward signal constructed by $F = G^{-1}$. Hence, feedforward control requires an accurate model of the inverse system. Next, it is highlighted where data-driven modeling using GPs contributes in feedforward control design.

2.2 The Potential of Gaussian Processes for Motion Control Applications The main focus in this paper is on the application of GPs for accurate motion control. Several different control applications are considered where feedforward plays a major role. In these examples, the application of a GP fits perfectly in the control scheme and leads to an increase in performance compared to traditional methods in advanced motion control applications. The examples considered in this paper are the following.

(1) The design of a feedforward $f = Fr$, see Fig. 1, where GPs are employed to represent the feedforward filter F in an appropriate manner. Both identification from input and output data and learning approaches [30] are covered, as well as extensions to nonlinear systems (Sec. 4).
(2) The design of a position-dependent feedforward where the GP models the dependency of the system parameters as a continuous function of position (Sec. 5).
(3) The design of feedforward signal f for certain classes of nonlinear systems where GPs are employed to represent the nonlinear inverse system based on input and output data (Sec. 6).
(4) The design of a repetitive control approach to compensate spatial disturbances that are not necessarily periodic in time. A GP is used to model a periodic position-domain function used to generate a compensatory signal (Sec. 7).

In Sec. 3, GPs are defined in view of their use in motion control.

3. Gaussian Processes for Motion Control Applications

GPs are at the heart of a very convenient mathematical framework for function estimation and interpolation. Function estimation is necessary when a model of a system contains some unknown function $g_0 : \mathcal{X} \to \mathbb{R}$, defined on some arbitrary domain $\mathcal{X}$, about which an accurate model g must be obtained from measurements. The function g_0 could,

e.g., represent the input of a system as a function of its output, the dependence of system parameters as a function of position, and periodic disturbances in a system as a function of position.

Such function estimation can be performed at least theoretically with a process called Bayesian inference: an initial guess of the unknown function is encoded as a probability distribution over functions, called the *prior* distribution, after which a few outcomes, or measurements, of the function are observed, and finally the prior distribution is conditioned on these outcomes to obtain the so-called *posterior* distribution. This a posterior distribution gives an estimate on the actual function in the system. In practice, however, it is often very difficult to compute the posterior distribution and often requires approximations [57].

Bayesian inference becomes *practical* when the prior distribution is required to be determined by a GP. Then, the posterior distribution is determined by a GP as well, and it is actually easy to compute the properties of this distribution. Moreover, the class of GPs is still rich enough so that in practice all kinds of unknown functions can successfully be modeled.

3.1 Definitions A GP is a collection of real-valued random variables $g(x)$ that are indexed by values x in some set $\mathcal{X}$, such that any finite number of them follows a multivariate Gaussian distribution. Here $\mathcal{X}$ can be just any set, for example $\mathbb{R}$.

A GP is fully specified by its mean $m : \mathcal{X} \to \mathbb{R}$ given by

$$m(x) := \mathbb{E}[g(x)], \quad \text{for } x \in \mathcal{X} \cdots\cdots (5)$$

and the covariance function, or kernel, $k : \mathcal{X} \times \mathcal{X} \to \mathbb{R}$

$$k(x, x') := \mathsf{Cov}(g(x), g(x')), \quad \text{for } x, x' \in \mathcal{X}. \cdots\cdots (6)$$

The notation

$$g(x) \sim \mathcal{GP}\left(m(x), k(x, x')\right), \cdots\cdots (7)$$

indicates that $(g(x))_{x\in\mathcal{X}}$ is a GP with mean function m and covariance function k.

3.2 Noisy Measurements Next, noisy measurements are obtained on the system to get more information about the unknown function $g_0 : \mathcal{X} \to \mathbb{R}$. A sequence

$$X = [x_1, \ldots, x_N] \cdots\cdots (8)$$

of training inputs in $\mathcal{X}$ is selected, and a sequence

$$Y = [y_1, \ldots, y_N] \cdots\cdots (9)$$

of noisy measurements is obtained of the GP at those input points. In the simplest case, this forms the basis of the computations below,

$$y_n := g(x_n) + \epsilon_n, \quad \text{for } n = 1, \ldots, N, \cdots\cdots (10)$$

where ϵ_n are i.i.d. normally distributed with mean 0 and standard deviation σ. Note that the whole framework can be generalized to a situation where the random variables $g(x)$ and y_n all together form a GP. One relevant example in relation to kernel-based regularization is where

$$y_n := L_n(g) + \epsilon_n \cdots\cdots (11)$$

for linear operators L_n.

3.3 Conditioning After obtaining noisy measurements $y_1, \ldots, y_N$, the process g is conditioned on these observations. Here, the GP $(g(x))_{x\in\mathcal{X}}$ after conditioning becomes a model for the real unknown function $g_0(x)$.

The key reasons for the broad success of GPs is the fact that the new mean and covariance function of this conditioned process can actually be computed easily. In particular, when conditioning a collection of jointly Gaussian random variables on a subset of them, the conditioned distribution is again Gaussian with tractable mean and covariance.

To describe the conditioned process, the conditioned (Gaussian) distribution of the conditioned variables $g(x)$ for $x \in X_*$ must be described for every finite subcollection of test inputs X_*. If the GP has covariance function $k : \mathcal{X} \times \mathcal{X} \to \mathbb{R}$, and

$$X_* := [x_{*,1}, \ldots, x_{*,M}] \cdots\cdots (12)$$

is some finite collection of inputs in $\mathcal{X}$, then the conditioned distribution for $(g(x))_{x\in X_*}$ is multivariate Gaussian with mean

$$\mu_* + K(X_*, X)(K(X, X) + \sigma^2 I)^{-1}(Y - \mu) \cdots\cdots (13)$$

and covariance

$$K(X_*, X_*) - K(X_*, X)(K(X, X) + \sigma^2 I)^{-1} K(X, X_*) \cdots\cdots (14)$$

where

$$\mu_* = \mathbb{E}[(g(x) : x \in X_*)], \cdots\cdots (15)$$
$$\mu = \mathbb{E}[(g(x) : x \in X)]. \cdots\cdots (16)$$

For Y and Z finite sequences in $\mathcal{X}$, the matrix $K(Y, Z)$ is defined by

$$K(Y, Z)_{ij} := k(y_i, z_j). \cdots\cdots (17)$$

The prior distribution, i.e., the GP before conditioning, is obtained for (7) with $x \in \mathcal{X}_*$. An example of 3 samples from this distribution with zero mean and the resulting posterior distribution after conditioning on 3 data points is shown in top row of Fig. 2.

3.4 Kernels The choice of kernel in the prior distribution is relevant as it can encode prior information such as the smoothness of the random function g. The quality of GP regression dependents on the user-selected selected kernel and hyper-parameters. As an example, see the bottom row of Fig. 2 where the hyper-parameter is selected less smooth. The latter can be optimised using Empirical Bayes, also referred to as marginal likelihood optimization, see, e.g., [31][33].

3.5 Gaussian Processes and Kernel-based Regularization GPs are intimately related to kernel-based regularization [58]. For kernels k which satisfy a condition called positive definiteness, an associated reproducing kernel Hilbert space $\mathcal{H}$ with corresponding norm $\|.\|_{\mathcal{H}}$ can be constructed. If the prior of the GP has zero mean, the solution μ_* found in (13) corresponds to $g(X_*)$ where $g : \mathcal{X} \to \mathbb{R}$ is the minimizer of the functional

$$J(g) := \|g(X) - Y\|_2^2 + \sigma^2 \|g\|_{\mathcal{H}}^2, \cdots\cdots (18)$$

see e.g. [58, Prop. 3.6] and [31, Sec. 6.2 and 6.2.2].

More generally, the mean of the posterior distribution of a

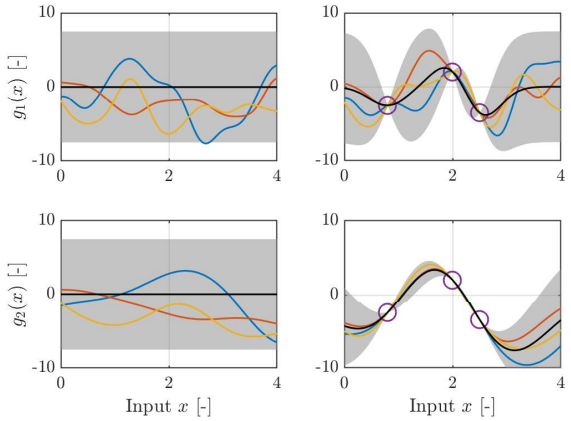

Fig. 2. Top left: 3 samples (—, —, —) drawn from the prior distribution with prior mean of zero (—) and uncertainty bounds ( ). Top right: posterior mean (—) of (13) after conditioning on 3 observations (o). The bottom row is the same as the top row except for a slight change in the kernel hyper-parameter related to smoothness. Note that the uncertainty of the posterior distribution (14) is low near the data points and that it heavily depends on the hyper-parameters

GP given measurements as in (11) is given by the minimum of

$$J(g) := \sum_{n=1}^{N} (L_n(g) - y_n)^2 + \sigma^2 \|g\|_{\mathcal{H}}^2, \cdots\cdots\cdots\cdots \quad (19)$$

which can be proven with similar methods as in [33, Sec. 12].

Conversely, a reproducing kernel Hilbert space $\mathcal{H}$, and a reproducing kernel $k : \mathcal{X} \times \mathcal{X} \to \mathbb{R}$ always induce a GP on $\mathcal{X}$. So starting with an optimization problem (18) or (19), there is always a GP that belongs to it, see, e.g., [58].

3.6 Uncertainty Estimation One of the benefits of Bayesian inference with GPs is that the framework gives an uncertainty estimate on the function value $g_0(x)$ for every x in the domain $\mathcal{X}$. This uncertainty estimate is encoded in the standard deviation of the random variable g_t after it is conditioned on the observations g. In summary, not only an estimate on the function g_0 is obtained, but it is also known for which input the estimate is likely accurate, and for which input the estimate is likely to be inaccurate.

3.7 Summary In summary, the above mechanics describe a continuous function estimation procedure using GPs. First, an appropriate prior is selected, where after it is conditioned on the measurement data to obtain the posterior distribution. Next, GPs are applied to relevant continuous functions in advanced motion control.

4. Gaussian Processes for Noncausal Feedforward

In this section, the design of a noncausal feedforward is described where GPs are employed to represent the inverse system dynamics. First, the problem setting for noncausal feedforward control is described. Second, a system identification approach using input and output data with noncausal kernels is presented, followed by an iterative learning approach with extensions to nonlinear systems. Third, experimental results are presented.

4.1 Problem Setting Consider Fig. 1 with the closed-loop tracking error defined in (3). Here, the goal is to design the feedforward controller F to reduce the tracking error. Recall from Sec. 2.1 that zero reference-induced tracking error is obtained for $F = G^{-1}$. Hence, feedforward control requires models of the inverse system.

If $G = \frac{B}{A}$ is a rational system, the exact feedforward controller $F = \frac{A}{B}$ is rational [30]. For non-minimum phase (NMP) systems, i.e., systems with zeros outside the unit circle, and for systems in the form of (1) feedforward signals are noncausal for exact tracking.

Independent of possible noncausality, identification of these noncausal systems is crucial in feedforward control and requires careful selection of model structure and order. Often, the model structure and order are selected based on physical insight, including mass and snap feedforward [15], or with regularization techniques to promote low-order models, see, e.g., [59].

The key idea in this section is to design noncausal feedforward signals, where the complexity is specified in a fundamentally different way through a noncausal impulse response representation based on a GP, as specified next.

4.2 Gaussian Processes for Open-loop Inverse Model Identification of Linear Systems In this section, the inverse model G^{-1} is represented by a noncausal impulse response. In particular, G^{-1} admits a bilateral z-transform, defined by two-sided formal Laurent series

$$G^{-1}(z) = \sum_{\tau=-\infty}^{\infty} \theta_\tau z^{-\tau}, \cdots\cdots\cdots\cdots\cdots\cdots\cdots\cdots \quad (20)$$

where $\theta = \{\theta_\tau\}_{\tau=\infty}^{\infty}$ is the impulse response, see [60, Thm. 1]. Note that (20) is bi-infinite due to the bilateral z-transform, which implies that G^{-1} is a noncausal and bounded operator, hence, $F = G^{-1}$ is noncausal. For noncausal feedforward the entire reference trajectory r must be known, which is often the case.

The key idea is to model the impulse response parameters θ of (20) as a zero-mean GP, using the relationship between kernel-based regression and GPs as described in Sec. 3.5. In fact, the starting point for the estimation of the impulse response parameters is the choice of an appropriate reproducing kernel Hilbert space $\mathcal{H}$ with positive definite kernel k. The kernel k specifies the underlying model complexity and regularizes the parameters, which can be exploited to impose prior knowledge and constraints, e.g., noncausality, stability, and, smoothness. See [60][61] for noncausal kernels and their relative performance for system identification and feedforward control.

As measurements, we consider the data-set $\mathcal{D} = \{y(t), u(t)\}_{t=1}^{N}$, where the input is $y(t)$ and the output $u(t)$. The optimization analogous to the minimization of (19) is then given by

$$\hat{\theta} = \underset{\theta \in \mathcal{H}}{\operatorname{argmin}} \sum_{t=1}^{N} \left(u(t) - \sum_{\tau=-\infty}^{\infty} \theta_\tau y(t-\tau) \right)^2 + \sigma^2 \|\theta\|_{\mathcal{H}}^2. \cdots\cdots\cdots\cdots\cdots\cdots \quad (21)$$

The minimizer of (21) follows from the representer theorem, see, e.g., [33, Thm. 3].

Under certain assumptions†, the noncausal inverse model

† Care should be taken in order for the series in (22) to converge.

G^{-1}, interpreted as a function from $\ell^2(\mathbb{Z}) \times \mathbb{Z}$ to $\mathbb{R}$, can itself be viewed as a GP $g : \ell^2(\mathbb{Z}) \times \mathbb{Z} \to \mathbb{R}$. The GP is then given by

$$g(y, t) := \sum_{\tau=-\infty}^{\infty} \theta_\tau y(t-\tau). \quad (22)$$

This links to Sec. 6 where the GP model for the inverse system is taken as a starting point.

In (20), only LTI and possibly noncausal feedforward is considered. In addition, the approach here, see [60], only allows for open-loop systems, i.e., $C = 0$ in Fig. 1. Extensions to nonlinear elements and closed-loop systems are investigated next.

4.3 Kernel-based ILC Approach for Systems with Nonlinearities Kernel-based ILC (KILC) approach exploits the use of noncausal kernels to regularize the noncausal impulse response parameters and learns these simultaneously with prescribed nonlinear basis functions in closed-loop. This is relevant for motion systems with linear mechanics subjected to friction, e.g., nonlinear Coulomb friction.

To this end, a feedforward parameterization for flexible noncausal feedforward for nonlinear systems is developed and is specified as

$$f_j = \Psi(r)\theta_j, \quad (29)$$

$$= \sum_{\tau=-n_{ac}}^{n_c} \theta_{l,\tau} r(t-\tau) + \sum_{i=1}^{n_{nl}} \phi_i(r)\theta_{nl,i}, \quad (30)$$

where $\theta_j = [\theta_l, \theta_{nl}]^\top \in \mathbb{R}^{n_\theta \times 1}$ with $n_\theta = n_{ac} + 1 + n_c + n_{nl}$, and $\Psi(r) \in \mathbb{R}^{N \times n_\theta}$, containing two distinct parts: a noncausal FIR parameterization part describing the LTI system as in (20), and the part with nonlinear basis functions $\phi_i(r)$ containing, for example, Coulomb friction by including $\mathrm{sign}(\dot{r})$. Note that traditional ILC [6] is recovered as a special case by setting $\Psi = I_N$, hence, $f_j = \theta_j$.

The feedforward parameters $\theta \in \mathbb{R}^{n_\theta}$ are learned in closed-loop using ILC. Recall (3), the error for trial, or iteration, j, under assumption of $r = r_j = r_{j+1}$, the error for trial $j+1$ is derived,

$$e_{j+1} = e_j - SG\Psi(r)(\theta_{j+1} - \theta_j) - S(v_{j+1} - v_j), \quad (31)$$

where SG is the impulse response matrix of the process sensitivity. The objective of feedforward control in the ILC context is to minimize the tracking error of the next trial, e_{j+1} of (31), by designing θ_{j+1} based on measured data of the previous trial, i.e., e_j and θ_j. Since the measurement noise is unknown and only a model $\widehat{SG}$ of SG is known, the actual optimization is defined as the minimization of

$$J(\theta_{j+1}) = \|e_j - \widehat{SG}\Psi(r)(\theta_{j+1} - \theta_j)\|_2^2 + \gamma\|\theta_{j+1}\|_K^2, \quad (32)$$

where $\gamma\|\theta\|_K^2 = \gamma\theta^\top K^{-1}\theta$ is the user-defined regularization term with positive definite matrix $K \in \mathbb{R}^{n_\theta \times n_\theta}$ and positive weight $\gamma \in \mathbb{R}$. Here, K can serve as a prior on the parameters and γ balances the penalty on the feedforward parameters with the error signal, i.e., the prior with respect to the data. The regularization enforces model complexity and noncausality to deal with NMP systems. The minimization in (32) relates to (19) and therefore the optimization can also be linked to Gaussian process inference.

A key step in the developed kernel structure is making the kernel K block-diagonal consisting of two distinct parts, as

$$K = \begin{bmatrix} K_l & 0 \\ 0 & K_{nl} \end{bmatrix}. \quad (33)$$

where K_l is a prior on the FIR parameters and K_{nl} a part

Iterative Learning Control

Iterative learning control (ILC) can learn optimal command inputs for repetitive tasks. Extensions include ILC with basis functions (ILCBF), that allow for learning under varying motion tasks. For elaboration on ILC and its applications, see, e.g., [11][26].

Consider the closed-loop scheme of Fig. 1. Now, an experiment, also called trial or iteration, is denoted with index j, and has length $N \in \mathbb{N}$ with reference $r_j \in \mathbb{R}^N$. For experiment j, the tracking error is given by

$$e_j = Sr_j - SGf_j, \quad (23)$$

where $S = (I + GC)^{-1}$, as defined in (4). The objective in ILC is to minimize the tracking error of the next experiment,

$$e_{j+1} = Sr_{j+1} - SGf_{j+1}. \quad (24)$$

For the assumption that $r_{j+1} = r_j = r$, i.e., r is constant, Sr is eliminated from (23) and (24), yielding the error propagation from trial j to trial $j+1$, i.e.,

$$e_{j+1} = e_j + SGf_j - SGf_{j+1}. \quad (25)$$

To allow for flexibility in the motion task, the feedforward signal is parameterized by a set of basis functions, denoted by $\Psi(r_j) \in \mathbb{R}^{N \times n_\theta}$, and feedforward parameters $\theta \in \mathbb{R}^{n_\theta}$, i.e.,

$$f_j = \Psi(r_j)\theta_j. \quad (26)$$

By selection of $\Psi(r_j)$ as a function of the reference, the feedforward signal becomes invariant under the motion task, i.e., if the reference changes the feedforward signal changes accordingly, see (23).

The objective in ILC is to minimize the predicted error of the next experiment $j+1$, denoted by $\hat{e}_{j+1}$, and is defined by the following cost function:

$$\mathcal{J}_j(\theta_{j+1}) := \left\| e_j + \widehat{SG}(f_j - \Psi(r_{j+1})\theta_{j+1}) \right\|_{W_e}^2 + \left\| \Psi(r_{j+1})\theta_{j+1} \right\|_{W_f}^2 + \left\| \Psi(r_{j+1})\theta_{j+1} - f_j \right\|_{W_{\Delta f}}^2 \quad (27)$$

where $W_e > 0$, $W_f, W_{\Delta f} \geq 0$, $\hat{e}_{j+1} = e_j + \widehat{SG}(f_j - \Psi(r_{j+1})\theta_{j+1})$ the predicted error for trial $j+1$ based on measurement e_j and f_j, and $\widehat{SG}$ a model of the real system SG. The optimal feedforward parameters $\theta_{j+1}^{\mathrm{opt}}$ minimizing this cost function, i.e., that minimize the error for the next experiment, are given by

$$\theta_{j+1}^{\mathrm{opt}} := \underset{\theta_{j+1}}{\mathrm{argmin}}\, \mathcal{J}_j(\theta_{j+1}). \quad (28)$$

Note that the solution can be computed analytically since (27) is quadratic in θ_{j+1}. Additionally, traditional ILC is recovered as a special case: $\Psi = I_N$, hence, $f_{j+1} = \theta_{j+1}$.

Fig. 3. Iterative Learning Control

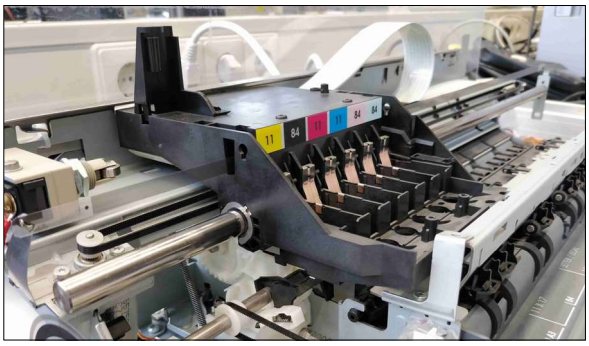

Fig. 4. Printer motion system with: motor, drive belt, slide guide, and carriage with printhead

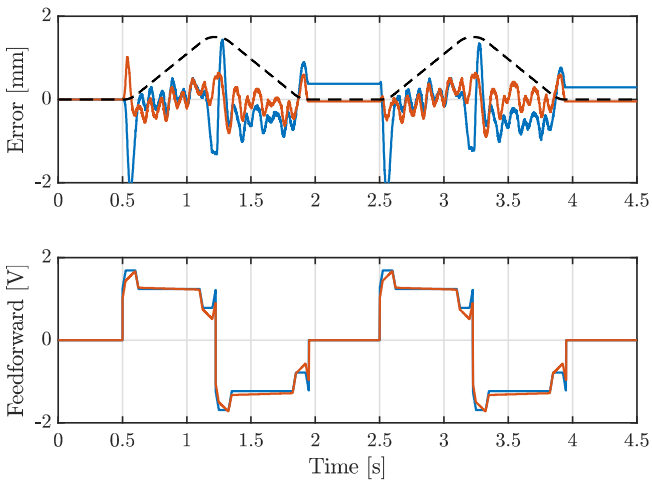

Fig. 5. Time-domain error and feedforward signals for the scaled reference (- -) of KILC using an OBF kernel (—) compared to ILCBF (—)

regularizing the nonlinear feedforward parameters, as described in (29). Note that norm-optimal ILC with basis functions (ILCBF) is recovered from KILC as a special case by setting $K = I_{n_\theta}$.

4.4 Experimental Results and Conclusion Initial results for positioning of a consumer printer, see Fig. 4, subject to nonlinear friction demonstrate the superior performance of KILC with 201 noncausal impulse response parameters and a noncausal orthogonal basis function (OBF) kernel [60] with pre-specified poles of the inverse system compared with ILCBF with acceleration as basis. Both methods also have a nonlinear Coulomb friction component. In Fig. 5, the time-domain error and feedforward signals are presented. The feedforward signal of KILC shows that it automatically identifies impulse response parameters to compensate higher-order dynamics, e.g., the snap parameter to compensate for the low-frequency contributions of the flexible dynamics [15].

In conclusion, noncausal kernels enforce model complexity and noncausality on the impulse response parameters to deal with NMP systems. Extension to iterative learning control and nonlinear basis functions allow accurate feedforward control in closed-loop for precision mechatronics.

5. Gaussian Processes for Position-dependent Parameterized Feedforward

This section describes the use of GPs to design position-dependent feedforward tuning, such as position-dependent snap feedforward. First, the problem for position-dependent feedforward is defined. Second, a method for parametrizing the feedforward signal in terms of the position using GPs and additionally an automated experiment design procedure using mutual information optimization are presented. Finally, results of both a simulation and experimental setup are shown.

5.1 Problem Setting Consider the dynamics seen in (1), i.e., a rigid-body mass with flexible connections. For the case at hand, the terms c_i and b_i are position-dependent, i.e., $c_i(x)$ and $b_i(x)$, where x is the position. The term $c_i(x)b_i^\top(x)$ is approximated by a position-dependent compliance term $D(x)$. This term is a continuous function of position due to, for example, parameter-varying resonance modes [62]. Typically, the term $D(x)$ or the structure thereof is unknown but smooth. To achieve zero reference-induced tracking error, i.e., $e = -Sv$, for position-dependent systems, the feedforward signal must be position-dependent, as follows from combining (1) and (3) and substituting $c_i(x)$ and $b_i(x)$.

In the remainder of this section, a feedforward parameterization, similar to (26), is considered. Here, it is assumed that the motion task r is short with respect to the position dependency, such that the position-dependent dynamics are excited primarily due to the initial position, i.e., considering *frozen* position-dependent dynamics. Next, the methods for using GPs to model feedforward parameters is presented.

5.2 Gaussian Processes for Position-dependent Snap Feedforward The compliance term $D(x)$, which is a continuous function of position, is compensated for by using snap feedforward [15], i.e., $f = \frac{\mathrm{d}^4 r}{\mathrm{d}t^4}\theta^s$. To achieve position-dependent snap feedforward, the snap parameter θ^s is now modeled as a function of position using a GP, $g(x)$, as in (7), i.e., $\theta^s(x) := g(x)$, see [63] for the original idea of modeling snap as a GP. In contrast to (26), the feedforward parameter $\theta^s(x)$ is now described by the GP as continuous function of the frozen position x. Hence, the feedforward signal for trial j and the frozen position x can be determined using

$$f_j(x) = \Psi(r_j)\theta_j(x) \cdots\cdots\cdots\cdots\cdots\cdots\cdots\cdots (34)$$

with appropriate selection of $\Psi(r_j)$ that includes $\frac{\mathrm{d}^4 r}{\mathrm{d}t^4}$ for snap feedforward. The GP of the snap feedforward parameter $\theta_j^s(x)$ that compensates for the position-dependent compliance $(D(x))_{x\in\mathcal{X}_*}$ for all given frozen positions X_* is given by (13) after conditioning on the data.

The observations, or data points, $(\theta_j(x_n))_{x_n\in\mathcal{X}}$ to condition the GP on, described by (10) can be obtained as follows. For different initial positions x, the optimal feedforward parameter $\theta_j(x)$ can be learned using, for example, ILCBF of Fig. 3. Note that a separate GP can be constructed for each position-dependent feedforward parameter, hence, for each feedforward parameter the resulting data-set is $\mathcal{D} = \{x_n, \theta_j(x_n)\}_{n=1}^N$. A difficulty is the selection of the initial positions X for conditioning, since these should be distributed optimally to identify the position-dependency with the least amount of data. To select the observation positions to reduce the estimation error, an approach based on mutual information (MI) optimization is proposed to position the observations near optimal [64].

Next, GPs for position-dependent feedforward is developed

Fig. 6. Commercial wirebonder from ASMPT consisting of an *xyz*-stage

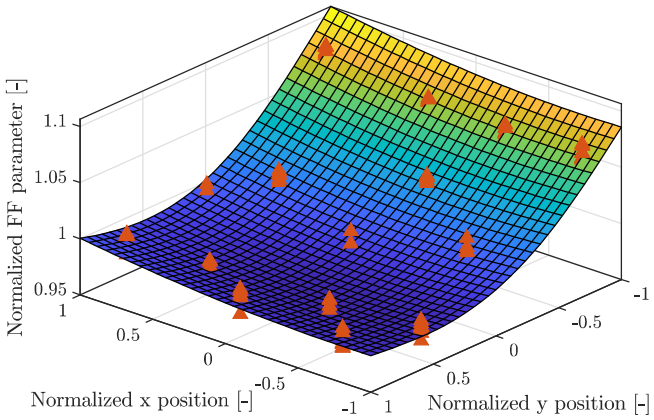

Fig. 8. Snap feedforward parameter θ^s of the z-axis modeled as a function of x, y-position by a GP for the experimental setup seen in Fig. 6. The observations (▲) are determined using ILCBF. Note that the GP models the position dependency as a smooth function of position and enables accurate interpolation

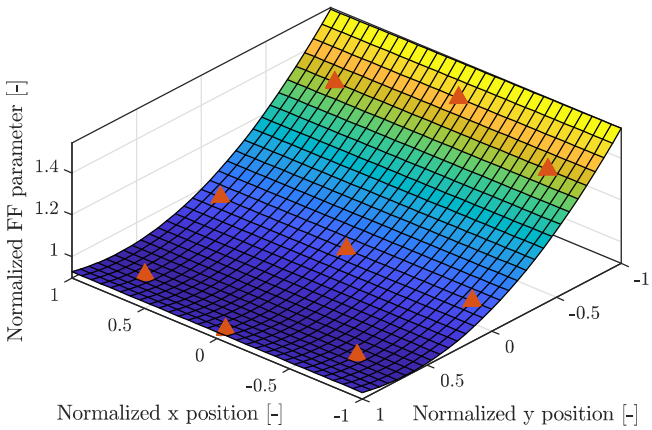

Fig. 7. Snap feedforward parameter θ^s of the x-axis modeled as a function of x, y-position by a GP in a simulation. The observations (▲) are determined using ILCBF and distributed near-optimally using MI optimization

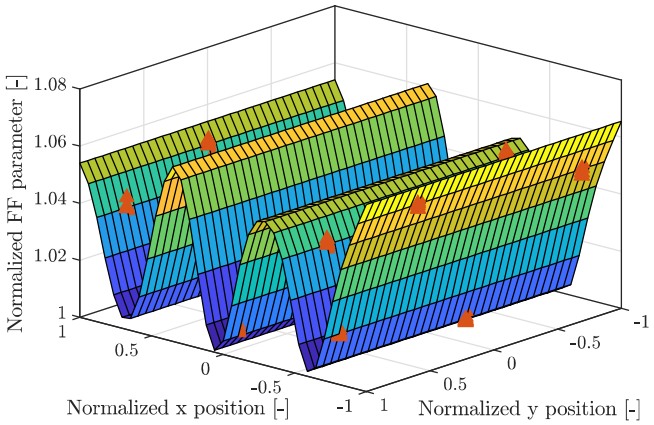

Fig. 9. Acceleration feedforward parameter θ^a of the x-axis modeled as a function of x, y-position by a GP for the experimental setup seen in Fig. 6. The observations (▲) are determined using ILCBF. The periodic effect of this feedforward parameter can be explained due to changing magnetic flux densities in the actuator

for an experimental setup and compared with a position-independent feedforward, i.e., ignoring the position dependency.

5.3 Experimental Results and Perspectives on Position-dependent Motor Constant Calibration Position-dependent feedforward using GPs is tested on a commercial wirebonder manufactured by ASMPT, consisting of three inputs and three outputs, i.e., x, y and z, see [65] for initial experimental results in this direction.

An example of a snap feedforward parameter as a function of the position in a simulation environment of a *xy*-stage of a wirebonder, can be seen in Fig. 7. The data points are determined using ILCBF, see Fig. 3, and show a clear dependency on the y position. The data points are near-optimally distributed over the *xy*-plane by optimization using mutual information optimization.

The feedforward parameters are modeled as a function of x, y position using a GP. Again, the observations are determined using ILCBF and MI optimization. The position-dependent snap feedforward parameter for the z-axis can be seen in Fig. 8. This method is also suitable for modeling other position-dependent effects, such as a position-dependent motor force constant or other feedforward parameters, illustrated by Fig. 9. Related experimental results are obtained in [66], yet in sharp contrast these variations are encoded as a prior.

Significant performance improvements are achieved compared to the traditional case when ignoring the position-dependent feedforward parameters, e.g. using a constant set of feedforward parameters, determined in the center position. This is illustrated by Fig. 10, which shows the error 2-norm for several different test positions for the x-axis and y-axis.

In summary, GPs enable the parameterization of feedforward parameters in terms of the position to reduce tracking errors due to position-dependent dynamics such as a position-dependent compliance or motor force constants. Mutual information is employed to automate experiment design by computing near-optimal data points such that the uncertainty and error of estimation of the feedforward parameters are reduced.

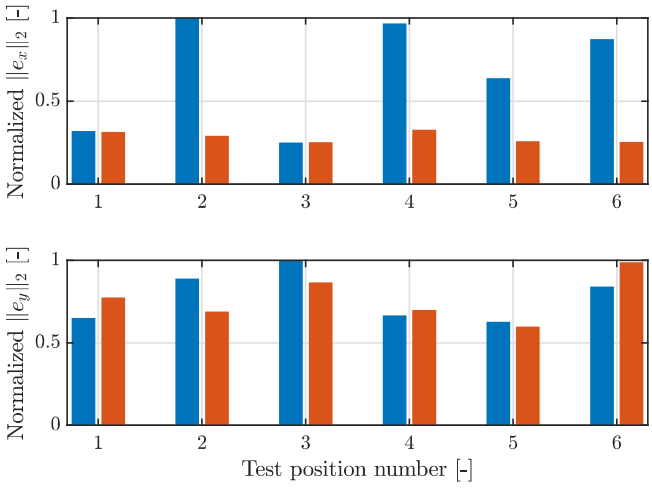

Fig. 10. Error 2-norm for several test positions for both GP position-dependent feedforward parameters ( ) and the feedforward parameters determined in the center position ( ). Clearly, a reduction in error 2-norm for multiple test positions is obtained using the GP position-dependent feedforward parameters

6. Gaussian Processes for Nonlinear Feedforward

In this section, the synthesis of feedforward signals for nonlinear systems, e.g., motion control systems with unknown nonlinearity, is considered by modeling the inverse system as a GP. In contrast to other GP-based feedforward approaches that learn a linear model G^{-1} [60] or learn a linear model with some pre-specified nonlinearity as seen in Sec. 4.3, the method described here requires no knowledge about the nonlinearity in the system. Moreover, the proposed method solely uses input and output data in contrast to the required Euler-Lagrange structure with known states in [43].

First, the problem setting is defined. Second, it is explained how GPs can be employed to construct feedforward signals from input-output data. Finally, the approach is applied to a consumer printer to demonstrate its ability to capture unknown nonlinear dynamics.

6.1 Problem Setting Here, a setting is assumed where G in Figure 1 is SISO and nonlinear. In particular, G^{-1} is assumed to be a noncausal nonlinear finite impulse response (NFIR) system, hence, nonlinear systems that require noncausal feedforward for perfect tracking are considered, see Sec. 4 for the motivation on noncausal feedforward. The NFIR is of the form

$$G^{-1} : u(t) = g(y_t) + \varepsilon_t, \quad t = 1, \ldots, N, \cdots\cdots\cdots\cdots (35)$$

where $y_t := [y(t+n_{ac}), \ldots, y(t-n_c)]^\top$, g is an unknown nonlinear function, and ε_t are i.i.d. normally distributed with mean 0 and standard deviation σ, see also [67] for a related approach. The scalars n_{ac} and n_c denote the number of anti-causal and causal samples, respectively. Note that (35) is equivalent to (10). Recall from Sec. 2.1 that zero reference-induced tracking error $e = r - y$ is achieved for $y = r$, i.e., $f(t) = g(r_t)$ in (35). The aim is then to obtain a model of g from data $\mathcal{D} = \{y(t), u(t)\}_{t=1}^{N}$, such that $f(t) = g(r_t)$ yields the feedforward signal required to realize reference r.

6.2 Approach The function $g(y)$ that describes the unknown nonlinear dynamics between input and output is now regarded as a GP, as defined in (7) with k a covariance function defining the smoothness of the function g. Consequently, by definition of g in (35), the kernel determines the smoothness of the required feedforward signal f for reference r. For instance, the Matèrn$_{3/2}$ covariance function can describe *non-smooth* nonlinear input-output behaviour accurately. The Matèrn$_{3/2}$ covariance function [31, p. 84] is constructed as

$$k(y, y') = \sigma_f^2(1 + \sqrt{3}\rho)\exp(-\sqrt{3}\rho), \cdots\cdots\cdots\cdots (36)$$

with $\rho = \sqrt{(y-y')^\top \Lambda^{-1}(y-y')}$, $\sigma_f^2 = \mathsf{Var}(f(y))$ and $\Lambda = \mathrm{diag}([\ell_1, \ldots, \ell_{n_c+n_{ac}+1}])$.

Next, the closed-loop measurement data-set $\mathcal{D} = \{Y, U\}$ is

$$Y = [y_1, \ldots, y_N], \cdots\cdots\cdots\cdots\cdots\cdots\cdots\cdots (37)$$
$$U = [u_1, \ldots, u_N], \cdots\cdots\cdots\cdots\cdots\cdots\cdots\cdots (38)$$

where $u_t = u(t)$ and $y_t = [y(t+n_{ac}), \ldots, y(t-n_c)]^\top$. The feedforward signal $f \in \mathbb{R}^{N_r}$ required to realize reference r with length N_r can be computed from the GP after conditioning on the data-set. The feedforward signal is then given by the posterior mean of (13) using $X_* = R$ where $R = [r_1, \ldots, r_{N_r}]$ is a Toeplitz matrix constructed from $r \in \mathbb{R}^{N_r}$, with $r_t := [r(t+n_{ac}), \ldots, r(t-n_c)]^\top$. Thus, the GP enables interpolation from Y to R.

Since a Matèrn$_{3/2}$ covariance function parameterizes a model in terms of distance to observations, see definition of ρ in (36), observations of $y_t \in \mathcal{D}$ close to $r_t \in R$ are required, where proximity is defined by the distance ρ. These observations of y and u are collected using closed-loop experiments. These experiments require careful selection of several excitation references, as well as a feedback controller C and the best available feedforward controller F, such that interpolation from Y to R in $n_c + n_{ac} + 1$ dimensions is possible. An example of this approach to a printer setup with nonlinear friction is demonstrated next.

6.3 Experimental Results Consider the printer in Figure 4. A feedback controller C is already implemented, as well as an existing feedforward F in the form of (26), with velocity and acceleration feedforward. Data is collected in 11 closed-loop experiments, during which the excitation references are chosen as scaled variations of the reference, see Fig. 11. The GP is conditioned on the data-set and is used to construct a feedforward signal with (13). The kernel hyperparameters σ_f, ℓ_i and σ are found by optimization of the marginal likelihood, see Sec. 3.4. The resulting error and feedforward signal are shown in Fig. 12, compared with the results of the original feedforward controller F. The 2-norm of the error is reduced by a factor 2.5 as a result of nonlinear GP-based feedforward. Indeed, by viewing G^{-1} as a GP in the form of (7), unknown nonlinear dynamics such as static friction can learned from input-output data.

7. Gaussian Processes for Position-dependent Disturbances

In this section, a disturbance rejection problem during continuous operation is considered, which is in contrast to the previously introduced tracking problems in batch-to-batch operation. More specifically, a GP-based spatial internal

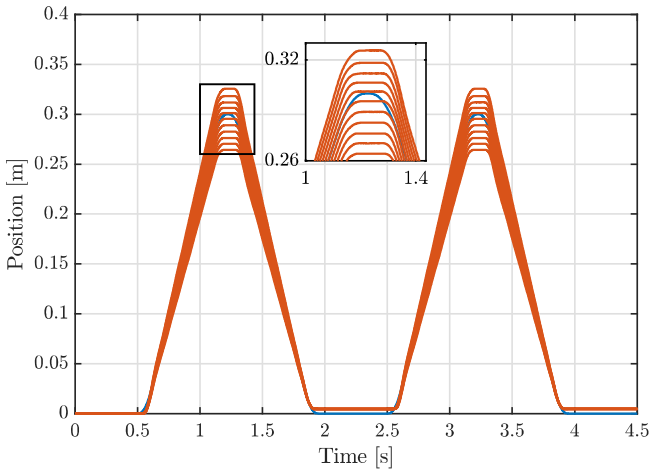

Fig. 11. Reference (—) and observed outputs (—) from closed-loop experiments with 11 different excitation references

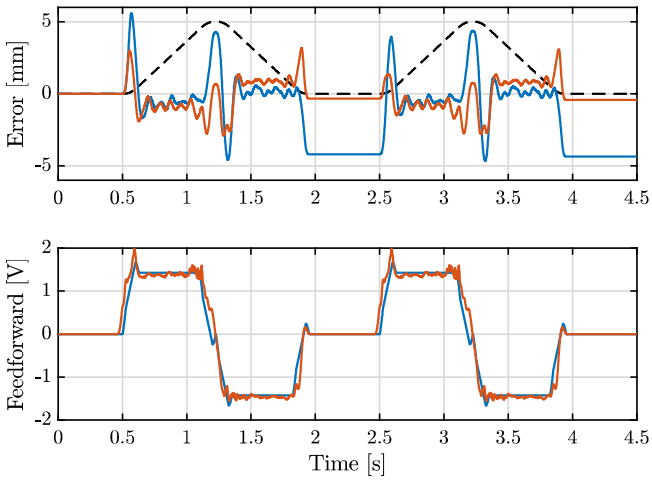

Fig. 12. Time-domain error and feedforward signals for the scaled reference (- -) using nonlinear GP-based feedforward (—), compared to ILCBF with acceleration and velocity as basis (—). The error is significantly reduced as a result of nonlinear GP-based feedforward

model for Repetitive Control (RC) is developed to compensate for disturbances that are repeating in the position domain, see [68] for preliminary results in this direction.

7.1 Position-domain Disturbance Rejection Problem

Consider the setting in Fig. 1 with $F = 0$, i.e., without feedforward, and where an input disturbance $d(t)$ is present that is given by

$$d(t) = \bar{d}_p(p(t)), \cdots\cdots\cdots\cdots\cdots\cdots\cdots\cdots\cdots\cdots (39)$$

where $p(t) \in \mathbb{R}$ is an exogenous position signal, and $\bar{d}_p$ is a periodic position-domain function, i.e.,

$$\bar{d}_p(p) = \bar{d}_p(p + i \cdot p_{\text{per}}), \quad \text{for } i \in \mathbb{N}, \cdots\cdots\cdots\cdots (40)$$

with $p_{\text{per}} \in \mathbb{R}$ the spatial period. Depending on the evolution of $p(t)$ the disturbance (39) may appear periodic or non-period in time.

Traditional RC employs the internal model principle to enable the asymptotic rejection of time-domain periodic disturbance with a fixed and known period time, see, e.g., [69]–[71]. However, the spatial disturbance $d(t)$ is not necessarily periodic in time if the velocity changes, consequently traditional

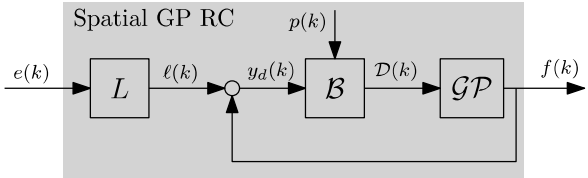

Fig. 13. GP-based repetitive controller

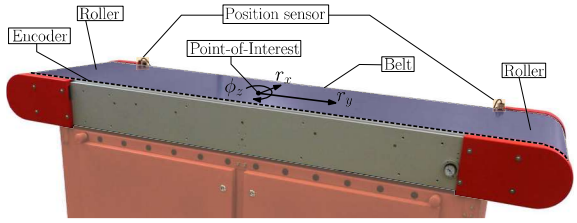

Fig. 14. Substrate carrier setup

temporal RC is not directly applicable. In the following section, a spatial internal model for RC is developed by modeling the function (40) as a GP, consequently, spatial RC can asymptotically compensate for $d(t)$ independent of the evolution of $p(t)$.

7.2 Spatial GP RC Approach

The GP-based spatial RC is depicted in Fig. 13, where L is a learning filter, and $\mathcal{B}$ a buffer that generates the data-set $\mathcal{D} = \{p_n, y_{d,n}\}_{n=1}^{N}$ that in general is non-equidistantly distributed in the position domain. The GP-based disturbance model used for compensation is represented by $\mathcal{GP}$.

The position-domain periodic disturbance $\bar{d}_p(p)$ is modeled as a GP of the form (7) where $x = p$ with zero mean and with a periodic covariance function

$$k(p, p') = \sigma_f^2 \exp\left(\frac{-2\sin^2(\frac{\pi(p-p')}{\lambda})}{l^2}\right), \cdots\cdots\cdots\cdots (41)$$

where λ is ideally equal to the period p_{per}, l is the characteristic length scale defining smoothness, and σ_f^2 a gain.

To compensate for the disturbance at time $t(k)$, the GP is conditioned on the data-set $\mathcal{D}$ with $p(k) \in \mathcal{X}_*$ to determine the compensation signal $f(k)$ that is given by the posterior mean as in (13).

7.3 Experimental Results

Spatial RC is validated on the experimental substrate carrier setup in Fig. 14 which is used for accurate transportation of various substrates for printing. The setup consists of a steel belt that rotates around two rollers, and each roller contains three segments for lateral belt positing. The imperfections in the rollers induce disturbances that are repeating in the roller-position domain. This can be seen in the cumulative power spectrum (CPS) of the error in the r_z-direction as a function of the spatial frequency, see Fig. 15 in (—), where a clear contribution is observed at 1 [1/rev] and 3 [1/rev].

By employing GP-based spatial RC with period $\lambda = 2\pi$, these contributions are completely removed from the error, see (—) in Fig. 15. In addition, the 2-norm of the error is shown in Fig. 16, where the roller velocity is changes indicated by the gray area (▬). This shows the error with spatial RC (×) is not influenced by the changing velocity, in contrast to traditional RC (×) where the error significantly increases if the velocity is changed.

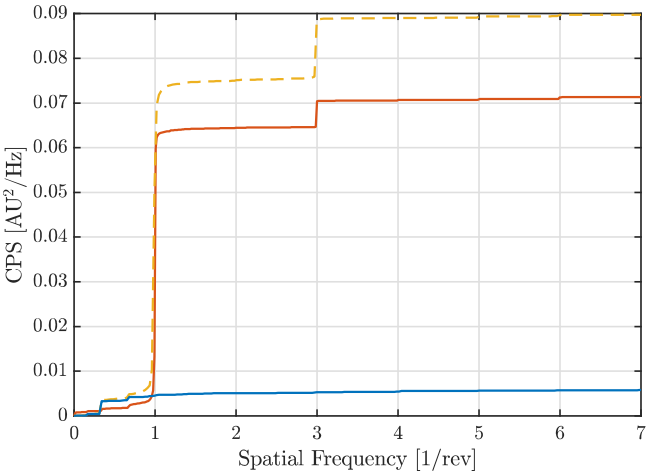

Fig. 15. Cumulative power spectrum (CPS) of the error as function of the spatial frequencies for PD control (—) indicating clear contributions at the 1 and 3 roller revolutions. Using GPRC these contributions are completely removed (—), whereas traditional RC even amplifies the spatial disturbance (- -) if the velocity changes

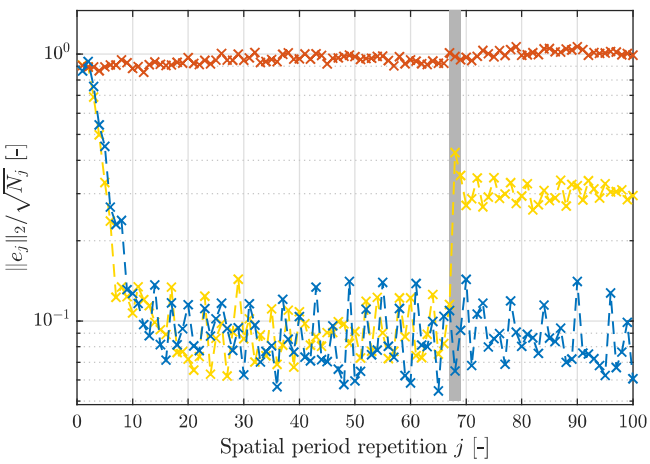

Fig. 16. 2-norm of the error scaled with the $\sqrt{N}$ for the PD controller (×) Spatial RC (×) and traditional RC (×). The gray area (▬) indicates where the belt velocity changes, showing the benefit of spatial RC where the performance is unaffected, whereas the traditional RC performance degrades due to inadequate buffer size after the velocity change

8. Conclusion and Outlook

Future data-intensive mechatronic systems benefit greatly from techniques that can fully exploit the information present in these data. Gaussian processes are one example of algorithms that are nonparametric and highly successful in the area of machine learning. It is shown that Gaussian processes are at the heart of a very convenient mathematical framework for function estimation and interpolation. The benefits are the inclusion of prior knowledge in a prior distribution and the inference on observations to obtain a posterior distribution with uncertainty estimate. The wide variety of use cases of Gaussian processes presented in this paper confirm that Gaussian processes significantly improve the accuracy of mechatronic systems by learning from data in a user-friendly manner. Successful applications include noncausal and nonlinear feedforward on a printer system, position-dependent feedforward on a wirebonder, and spatial repetitive control of a substrate carrier setup, and result in significant improvement in terms of accuracy.

Current research focuses on several aspects. First, Gaussian processes are being further deployed towards industrial applications. Second, fundamental developments include the use Gaussian processes in control techniques, including new repetitive control algorithms [72]. Third, other techniques that are at the intersection of control, machine learning, and mechatronics are being developed, including parametric techniques such as physics-guided neural networks [73], sparse optimisation for subset selection in feedforward and learning [59], and reinforcement learning for model-free learning in mechatronics [74].

Acknowledgment

The authors would like to thank Gert Witvoet, Lennart Blanken, Robin van Es, Dragan Kostić, and former master students for their contributions to this research. This paper contains a survey of contributions from different applications. The authors gratefully acknowledge the following support. The contributions of Van Haren and Van Meer related to Sec. 5 and 6, respectively, were carried out when they were affiliated with ASM Pacific Technology. They are currently PhD candidates within the ECSEL Joint Undertaking under grant agreement 101007311 (IMOCO4.E). The Joint Undertaking receives support from the European Union's Horizon 2020 research and innovation programme. The research of Mooren related to Sec. 7 was carried out within the IMOCO4.E consortium and received funding from the European Union H2020 program under grant agreement 637095 (FourByThree), and ECSEL-2016-1 under grant agreement 737453 (I-MECH). The research of Poot related to Sec. 4.3 is supported by ASM Pacific Technology. Moreover, the work in this paper is part of research programme VIDI with project number 15698, which is (partly) financed by the Netherlands Organisation for Scientific Research (NWO).

References

(1) K. Ohnishi, M. Shibata, and T. Murakami: "Motion control for advanced mechatronics", *IEEE/ASME Trans. Mech.*, Vol.1, No.1, pp.56–67 (1996)

(2) M. Steinbuch and M.L. Norg: "Industrial perspective on robust control: Application to storage systems", *Annual Reviews in Control*, Vol.22, pp.47–58 (1998)

(3) L. Ljung: System Identification: Theory for the User, Prentice Hall, Upper Saddle River, NJ, USA, second edition (1999)

(4) R. Pintelon and J. Schoukens: System Identification: A Frequency Domain Approach, IEEE Press, New York, NY, USA, second edition (2012)

(5) H. Hjalmarsson: "From experiment design to closed-loop control", *Automatica*, Vol.41, pp.393–438 (2005)

(6) D.A. Bristow, M. Tharayil, and A.G. Alleyne: "A survey of iterative learning control: A learning-based method for high-performance tracking control", *Contr. Syst. Mag.*, Vol.26, No.3, pp.96–114 (2006)

(7) T. Oomen, R. van Herpen, S. Quist, M. van de Wal, O. Bosgra, and M. Steinbuch: "Connecting system identification and robust control for next-generation motion control of a wafer stage", *IEEE Trans. Contr. Syst. Techn.*, Vol.22, No.1, pp.102–118 (2014)

(8) G. Cherubini, C.C. Chung, W.C. Messner, and S.O.R. Moheimani: "Control methods in data-storage systems", *IEEE Trans. Contr. Syst. Techn.*, Vol.20, No.2, pp.296–322 (2012)

(9) J. Bolder, J. van Zundert, S. Koekebakker, and T. Oomen: "Enhancing flatbed printer accuracy and throughput: Optimal rational feedforward controller tuning via iterative learning control", *IEEE Trans. Ind. Electr.*, Vol.64, No.5, pp.4207–4216 (2017)

(10) R.G. Landers, K. Barton, S. Devasia, T. Kurfess, P. Pagilla, and M. Tomizuka: "A review of manufacturing process control", *Journal of Manufacturing Science and Engineering*, Vol.142, No.11, p.110814 (2020)

(11) F. Boeren, A. Bareja, T. Kok, and T. Oomen: "Frequency-domain ILC approach for repeating and varying tasks: With application to semiconductor bonding equipment", *IEEE/ASME Trans. Mech.*, Vol.21, No.6, pp.2716–2727 (2016)

(12) S. Devasia, E. Eleftheriou, and S. Moheimani: "A survey of control issues in nanopositioning", *IEEE Trans. Contr. Syst. Techn.*, Vol.15, No.5, pp.802–823 (2007)

(13) R. Findeisen, M.A. Grover, C. Wagner, M. Maiworm, R. Temirov, F.S. Tautz, M.V. Salapaka, S. Salapaka, R.D. Braatz, and S.O.R. Moheimani: "Control on a molecular scale: a perspective", In *Proc. 2016 Americ. Contr. Conf.*, pp.3069–3076, Boston, MA, USA (2016)

(14) T. Oomen: "Advanced motion control for precision mechatronics: Control, identification. and learning of complex systems", *IEEJ Transactions on Industry Applications*, Vol.7, No.2, pp.127–140 (2018)

(15) M. Boerlage, R. Tousain, and M. Steinbuch: "Reference trajectory relevant jerk derivative feedforward control for motion systems", In *Proc. 2004 Americ. Contr. Conf.*, pp.4843–4848, Boston, MA, USA (2004)

(16) M. Steinbuch, R. van de Molengraft, and A.-J. van der Voort: "Experimental modelling and LPV control of a motion system", In *Proc. 2003 Americ. Contr. Conf.*, pp.1374–1379, Denver, CO, USA (2003)

(17) Z. Jamaludin, H. Van Brussel, and J. Swevers: "Friction compensation of an XY feed table using friction-model-based feedforward and an inverse-model-based disturbance observer", *IEEE Trans. Ind. Electr.*, Vol.56, No.10, pp.3848–3853 (2009)

(18) M. Ruderman and M. Iwasaki: "Observer of nonlinear friction dynamics for motion control", *IEEE Trans. Ind. Electr.*, Vol.62, No.9, pp.5941–5949 (2015)

(19) N. Strijbosch and T. Oomen: "Hybrid-MEM-element feedforward: With application to hysteretic piezoelectric actuators", In *Proc. 59th Conf. Dec. Contr.*, pp.934–939, Jeju Island, Korea (2020)

(20) H. Hjalmarsson and K. Lindqvist: "Identification for control: l_2 and l_∞ methods", In *Proc. 40th Conf. Dec. Contr.*, pp.2701–2706, Orlando, FL, USA (2001)

(21) M. Steinbuch, J. van Helvoort, W. Aangenent, B. de Jager, and R. van de Molengraft: "Data-based control of motion systems", In *Proc. 2005 Americ. Contr. Conf.*, pp.529–534, Toronto, Canada (2005)

(22) M.F. Heertjes, N. Irigoyen Perdiguero, and D.A. Deenen: Robust control and data-driven tuning of a hybrid integrator-gain system with applications to wafer scanners, *Int. J. Adapt. Contr. Sign. Proc.*, Vol.33, pp.371–387 (2019)

(23) R. Voorhoeve, A. van der Maas, and T. Oomen: "Non-parametric identification of multivariable systems: A local rational modeling approach with application to a vibration isolation benchmark", *Mech. Syst. Sign. Proc.*, No.105, pp.129–152 (2018)

(24) R. Voorhoeve, R. de Rozario, W. Aangenent, and T. Oomen: "Identifying position-dependent mechanical systems: A modal approach with applications to wafer stage control", *IEEE Trans. Contr. Syst. Techn.*, Vol.29, No.1, pp.194–206 (2021)

(25) R.W. Longman: "Iterative learning control and repetitive control for engineering practice", *Int. J. Contr.*, Vol.73, No.10, pp.930–954 (2000)

(26) T. Oomen: "Learning for advanced motion control", In *Int. Workshop on Advanced Motion Contr.*, pp.65–72, Agder, Norway (2020)

(27) X. Chen and M. Tomizuka: "New repetitive control with improved steady-stage performance and accelerated transient", *IEEE Trans. Contr. Syst. Techn.*, Vol.22, No.2, pp.664–675 (2014)

(28) D.J. Hoelzle, A.G. Alleyne, and A.J. Wagoner Johnson: "Basis task approach to iterative learning control with applications to micro-robotic deposition", *IEEE Trans. Contr. Syst. Techn.*, Vol.19, No.5, pp.1138–1148 (2011)

(29) S. van der Meulen, R.L. Tousain, and O.H. Bosgra: "Fixed structure feedforward controller design exploiting iterative trials: Application to a wafer stage and a desktop printer", *J. Dyn. Syst., Meas., and Contr.*, Vol.130, pp.051006–1 (2008)

(30) L. Blanken, F. Boeren, D. Bruijnen, and T. Oomen: "Batch-to-batch rational feedforward control: from iterative learning to identification approaches, with application to a wafer stage", *IEEE/ASME Trans. Mech.*, Vol.22, No.2, pp.826–837 (2017)

(31) C.E. Rasmussen and C.K.I. Williams: "Gaussian Processes for Machine Learning", Massachusetts Institute of Technology (2006)

(32) M.P. Deisenroth, D. Fox, and C.E. Rasmussen: "Gaussian processes for data-efficient learning in robotics and control", *IEEE Transactions on Pattern Analysis and Machine Intelligence*, Vol.37, No.2, pp.408–423 (2015)

(33) G. Pillonetto, F. Dinuzzo, T. Chen, G. De Nicolao, and L. Ljung: "Kernel methods in system identification, machine learning and function estimation: A survey", *Automatica*, Vol.50, No.3, pp.657–682 (2014)

(34) L. Ljung, T. Chen. and B. Mu: "A shift in paradigm for system identification", *Int. J. Contr.*, Vol.93, No.2, pp.173–180 (2019)

(35) J. Kocijan: "Modelling and Control of Dynamic Systems Using Gaussian Process Models", Advances in Industrial Control. Springer, Switzerland (2016)

(36) M. Darwish, P. Cox, I. Proimadis, G. Pillonetto, and R. Tóth: "Prediction-error identification of lpv systems: A nonparametric gaussian regression approach", *Automatica*, Vol.97, pp.92–103 (2018)

(37) J. Lataire and T. Chen: "Transfer function and transient estimation by gaussian process regression in the frequency domain", *Automatica*, Vol.72, pp.217–229 (2016)

(38) S. Devasia: "Iterative machine learning for output tracking", *IEEE Trans. Contr. Syst. Techn.*, Vol.27, No.2, pp.516–526 (2019)

(39) A. Jain, T.X. Nghiem, M. Morari, and R. Mangharam: "Learning and control using Gaussian processes: Towards bridging machine learning and controls for physical systems", In *2018 9th ACM/IEEE International Conference on Cyber-Physical Systems*, pp.140–149, Porto, Portugal (2018)

(40) M. Greeff and A.P. Schoellig: "Exploiting differential flatness for robust learning-based tracking control using Gaussian processes", *IEEE Contr. Syst. Lett. (L-CSS)*, Vol.5, No.4, pp1121–1126 (2021)

(41) L. Hewing, J. Kabzan, and M.N. Zeilinger: "Cautious model predictive control using gaussian process regression", *IEEE Trans. Contr. Syst. Techn.*, Vol.28, No.6, pp.2736–2743 (2020)

(42) G. Männel, J. Graßhoff, P. Rostalski, and H. Abbas: "Iterative gaussian process model predictive control with application to physiological control systems", In *Proc. 60th Conf. Dec. Contr.*, pp.2203–2210, Austin, TX, USA (2021)

(43) T. Beckers, D. Kulić, and S. Hirche: "Stable Gaussian process based tracking control of Euler-Lagrange systems", *Automatica*, Vol.103, pp.390–397 (2019)

(44) H. Bijl: "LQG and Gaussian process techniques: For fixed-structure wind turbine control", PhD thesis, Delft University of Technology, Delft, The Netherlands (2018)

(45) J. Hendriks, N. O'Dell, A. Wills, A. Tremsin, C. Wensrich, and T. Shinohara: "Bayesian non-parametric bragg-edge fitting for neutron transmission strain imaging", *The Journal of Strain Analysis for Engineering Design*, Vol.56, No.6, pp.371–385 (2021)

(46) M. Kok and A. Solin: "Scalable magnetic field SLAM in 3D using Gaussian process maps", In *Proceedings of the 20th International Conference on Information Fusion*, Cambridge, UK (2018)

(47) L. Sforni, I. Notarnicola, and G. Notarstefano: "Learning-driven nonlinear optimal control via gaussian process regression", In *Proc. 60th Conf. Dec. Contr.*, pp.4412–4417, Austin, TX, USA (2021)

(48) F. Castañeda, J. Choi, B. Zhang, C. Tomlin, and K. Sreenath: "Pointwise feasibility of gaussian process-based safety-critical control under model uncertainty", In *Proc. 60th Conf. Dec. Contr.*, Austin, TX, USA (2021)

(49) R. Munnig Schmidt, G. Schitter, and J. van Eijk: *The Design of High Performance Mechatronics*, Delft University Press, Delft, The Netherlands (2011)

(50) A.J. Fleming: "Measuring and predicting resolution in nanopositioning systems", *Mechatronics*, Vol.24, No.6, pp.605–618 (2014)

(51) W.K. Gawronski: *Advanced Structural Dynamics and Active Control of Structures*, Springer, New York, NY, USA (2004)

(52) P.C. Hughes: "Space structure vibration modes: How many exist? Which ones are important?", *IEEE Contr. Syst. Mag.*, Vol.7, No.1, pp.22–28 (1987)

(53) A.J. Fleming and K.K. Leang: *Design, Modeling and Control of Nanopositioning Systems*, Springer (2014)

(54) T. Oomen, E. Grassens, and F. Hendriks: "Inferential motion control: An identification and robust control framework for unmeasured performance variables", *IEEE Trans. Contr. Syst. Techn.*, Vol.23, No.4, pp.1602–1610 (2015)

(55) P. Lambrechts, M. Boerlage, and M. Steinbuch: "Trajectory planning and feedforward design for electromechanical motion systems", *Contr. Eng. Prac.*, Vol.13, pp.145–157 (2005)

(56) E. de Gelder, M. van de Wal, C. Scherer, C. Hol, and O. Bosgra: "Nominal and robust feedforward design with time domain constraints applied to a wafer stage", *J. Dyn. Syst., Meas., and Contr.*, Vol.128, No.2, pp.204–215 (2006)

(57) C. Robert and G. Casella: *Monte Carlo Statistical Methods*, Springer-Verlag New York (2004)

(58) M. Kanagawa, P. Hennig, D. Sejdinovic, and B.K. Sriperumbudur: "Gaussian processes and kernel methods: A review on connections and equivalences", *eprint arXiv:1807.02582* (2018)

(59) T. Oomen and C.R. Rojas: "Sparse iterative learning control with application to a wafer stage: Achieving performance, resource efficiency, and task flexibility", *Mechatronics*, Vol.47, pp.134–137 (2017)

(60) L. Blanken and T. Oomen: "Kernel-based identification of non-causal

systems with application to inverse model control", *Automatica*, Vol.114, p.108830 (2020)

(61) R.A. González, C.R. Rojas, and H. Hjalmarsson: "Non-causal regularized least-squares for continuous-time system identification with band-limited input excitations", In *Proc. 60th Conf. Dec. Contr.*, pp.114–119 (2021)

(62) R. de Rozario, and T. Oomen: "Frequency response function identification of periodically scheduled linear parameter-varying systems", *Mech. Syst. Sign. Proc.*, Vol.148, p.107156 (2021)

(63) M. van Haren, M. Poot, J. Portegies, and T. Oomen: "Position-dependent snap feedforward: A gaussian process framework", In *Proc. 2022 Americ. Contr. Conf.*, Atlanta, GA, USA (2022)

(64) A. Krause: "Near-optimal sensor placements in Gaussian processes: Theory, efficient algorithms and empirical studies", *Journal of Machine Learning Research*, Vol.9, pp.235–284 (2008)

(65) M. van Haren, M. Poot, D. Kostić, R. van Es, J. Portegies, and T. Oomen: Gaussian process position-dependent feedforward: With application to a wire bonder, In *Int. Workshop on Advanced Motion Contr.* (2022)

(66) I. Proimadis, Y. Broens, R. Tóth, and H. Butler: "Learning-based feedforward augmentation for steady state rejection of residual dynamics on a nanometer-accurate planar actuator system", In *Proceedings of Machine Learning Research*, Vol.144, pp.1–12 (2021)

(67) J. Lee and S. Oh: "Data-based design of inverse dynamics using gaussian process", In *IEEE Int. Conf. Mech.*, Vol.1, pp.449–454 (2019)

(68) N. Mooren, G. Witvoet, and T. Oomen: "Gaussian process repetitive control for suppressing spatial disturbances", *IFAC-PapersOnLine*, Vol.53, No.2, pp.1487–1492 (2020)

(69) B. Francis and W. Wonham: "The internal model principle of control theory", *Automatica*, Vol.12, No.5, pp.457–465 (1976)

(70) G. Goodwin and K. Sin: *Adaptive filtering prediction and control*, Courier Corporation (2014)

(71) S. Hara, Y. Yamamoto, T. Omata, and M. Nakano: "Repetitive control system: A new type servo system for periodic exogenous signals", *IEEE Transactions on Automatic Control*, Vol.33, No.7, pp.659–668 (1988)

(72) N. Mooren, G. Witvoet, and T. Oomen: "Gaussian process repetitive control: Beyond periodic internal models through kernels", *To appear in Automatica* (2022)

(73) J. Kon, D. Bruijnen, J. van de Wijdeven, M. Heertjes, and T. Oomen: "Physics-guided neural networks for feedforward control: An orthogonal projection-based approach", In *Proc. 2022 Americ. Contr. Conf.*, Atlanta, GA, USA (2022)

(74) M. Poot, J. Portegies, and T. Oomen: "On the role of models in learning control: Actor-critic iterative learning control", In *IFAC 21st Triennial World Congress*, pp.1476–1481, Berlin, Germany (2020)

Maurice Poot (Non-member) received the M.Sc. degree from the Eindhoven University of Technology, Eindhoven, The Netherlands in 2019. He is currently a Ph.D. candidate at the Eindhoven University of Technology in the Department of Mechanical Engineering. His research interests include Gaussian processes, data-driven learning, learning, and control with application to mechatronic systems.

Jim Portegies (Non-member) obtained his M.Sc. degree in Industrial and Applied Mathematics and Applied Physics from the Eindhoven University of Technology in 2009. He spent the 2007–2008 academic year as an exchange student at the University of Bonn, Germany. He received his Ph.D. degree in Mathematics from the Courant Institute of Mathematical Sciences in New York. In the Fall of 2013, he spent a semester at NYU Shanghai, in Shanghai, China. After completing his Ph.D. in 2014, he spent two years a postdoc at the Max Planck Institute for Mathematics in the Sciences in Leipzig, Germany until he returned to the Eindhoven University of Technology as an assistant professor in Mathematics in 2016.

Noud Mooren (Non-member) received his B.Sc. degree from Fontys University of Applied Sciences, and M.Sc. degree (cum laude) from the Eindhoven University of Technology, Eindhoven, The Netherlands. He is currently a Ph.D. candidate at the Eindhoven University of Technology. He is a recipient of the 2020 AMC Best Paper Award. His research interest is in the field of motion control and learning control techniques for applications in mechatronic systems.

Max van Haren (Non-member) received the M.Sc. degree (cum laude) in Systems and Control from the Eindhoven University of Technology, The Netherlands, in 2021. He is currently pursuing a Ph.D. degree in the Department of Mechanical Engineering at the Eindhoven University of Technology. His research interests include data-driven control and identification for complex mechatronic systems.

Max van Meer (Non-member) received his M.Sc. degree (cum laude) in Mechanical Engineering from the Eindhoven University of Technology, Eindhoven, the Netherlands in 2021. He is currently a Ph.D. candidate at the Eindhoven University of Technology in the Department of Mechanical Engineering. His research interests include learning control, real-time systems and machine learning for motion control.

Tom Oomen (Non-member) received the M.Sc. degree (cum laude) and Ph.D. degree from the Eindhoven University of Technology, Eindhoven, The Netherlands. He is currently a professor with the Department of Mechanical Engineering at the Eindhoven University of Technology. He is also a part-time full professor with the Delft University of Technology. He held visiting positions at KTH, Stockholm, Sweden, and at The University of Newcastle, Australia. He is a recipient of the 7th Grand Nagamori Award, the Corus Young Talent Graduation Award, the IFAC 2019 TC 4.2 Mechatronics Young Research Award, the 2015 IEEE Transactions on Control Systems Technology Outstanding Paper Award, the 2017 IFAC Mechatronics Best Paper Award, the 2019 IEEJ Journal of Industry Applications Best Paper Award, and recipient of a Veni and Vidi personal grant. He is Associate Editor of the IEEE Control Systems Letters (L-CSS), IFAC Mechatronics, and IEEE Transactions on Control Systems Technology. He is a member of the Eindhoven Young Academy of Engineering. His research interests are in the field of data-driven modeling, learning, and control, with applications in precision mechatronics.